HHS Public Access

Author manuscript

J Clin Immunol. Author manuscript; available in PMC 2022 February 01.

Published in final edited form as:

J Clin Immunol. 2021 August ; 41(6): 1291–1302. doi:10.1007/s10875-021-01052-0.

Clinical Manifestations, Mutational Analysis, and Immunological Phenotype in Patients with *RAG1/2* Mutations: First Cases Series from Mexico and Description of Two Novel Mutations

Saul Oswaldo Lugo-Reyes[#1], **Nina Pastor**[#2], **Edith González-Serrano**[1], **Marco Antonio Yamazaki-Nakashimada**[1], **Selma Scheffler-Mendoza**[1], **Laura Berron-Ruiz**[1], **Guillermo Wakida**[1], **Maria Enriqueta Nuñez-Nuñez**[3], **Ana Paola Macias-Robles**[4], **Aide Tamara Staines-Boone**[5], **Edna Venegas-Montoya**[5], **Carmen Alaez-Verson**[6], **Carolina Molina-Garay**[6], **Luis Leonardo Flores-Lagunes**[6], **Karol Carrillo-Sanchez**[6], **Julie Niemela**[7], **Sergio D. Rosenzweig**[7], **Paul Gaytan**[8], **Jorge A. Yañez**[8], **Ivan Martinez-Duncker**[2], **Luigi D. Notarangelo**[7], **Sara Espinosa-Padilla**[1], **Mario Ernesto Cruz-Munoz**[9]

[1]Laboratorio de Inmunodeficiencias, Instituto Nacional de Pediatría, Mexico City, Mexico

[2]Centro de Investigación en Dinámica Celular, Universidad Autónoma del Estado de Morelos, Cuernavaca, Mexico

[3]Hospital Civil de Guadalajara Dr. Juan I. Menchaca, Guadalajara, Mexico

[4]Centro Medico Nacional de Oriente IMSS, Mexico City, Mexico

[5]Unidad Médica de Alta Especialidad 25, Instituto Mexicano del Seguro Social, Mexico City, Mexico

[6]Instituto Nacional de Medicina Genómica, Mexico City, Mexico

[7]Laboratory of Clinical Immunology and Microbiology, National Institute of Health, Mexico City, Mexico

[8]Instituto de Biotecnología, Universidad Nacional Autónoma de México, Mexico City, Mexico

[9]Facultad de Medicina, Universidad Autónoma del Estado de Morelos, Cuernavaca, Mexico

[#] These authors contributed equally to this work.

Abstract

Sara Espinosa-Padilla, saraelvaespino@gmail.com; Mario Ernesto Cruz-Munoz, mario.cruz@uaem.mx.

Author Contribution MECM and SEP conceived the study. MECM, SORL, and NP wrote the manuscript. SORL, JN, SDR, and LDN performed, analyzed, and interpreted the genetics. NP performed and analyzed the protein modeling. EGS and LBR performed proliferation assays and provided flow cytometry data. CAV, CMG, LLFL, and KCS provided the in silico analysis and classification of RAG1/2 variants. MAYN, SSM, GW, MENN, APMR, ATSB, and EVM took care of the patients and provided clinical data. PG and JAY performed genetic studies. IMD provided their expertise on congenital disorders. All authors critically reviewed the manuscript and approved the final version.

Supplementary Information The online version contains supplementary material available at https://doi.org/10.1007/s10875-021-01052-0.

Ethics Approval and Consent to Participate This study and the written consent forms were approved by the local ethics committees in accordance with the Declaration of Helsinki (Protocols 00165 and 049/2013).

Conflict of Interest The authors declare that they have no conflicts of interest.

Publisher's Note Springer Nature remains neutral with regard to jurisdictional claims in published maps and institutional affiliations.

Mutations in recombinase activating genes 1 and 2 (*RAG1/2*) result in human severe combined immunodeficiency (SCID). The products of these genes are essential for V(D)J rearrangement of the antigen receptors during lymphocyte development. Mutations resulting in null-recombination activity in RAG1 or RAG2 are associated with the most severe clinical and immunological phenotypes, whereas patients with hypomorphic mutations may develop leaky SCID, including Omenn syndrome (OS). A group of previously unrecognized clinical phenotypes associated with granulomata and/or autoimmunity have been described as a consequence of hypomorphic mutations. Here, we present six patients from unrelated families with missense variants in *RAG1* or *RAG2*. Phenotypes observed in these patients ranged from OS to severe mycobacterial infections and granulomatous disease. Moreover, we report the first evidence of two variants that had not been associated with immunodeficiency. This study represents the first case series of RAG1- or RAG2-deficient patients from Mexico and Latin America.

Keywords

Primary immunodeficiencies; RAG1/2; T lymphocytes; SCID; Omenn syndrome

Introduction

Human combined immunodeficiency (CID) comprises a group of inherited disorders that results from mutations in more than 50 genes that govern lymphocyte development, differentiation, and/or function [1-3]. Depending on severity, this group can be classified as severe combined immunodeficiency (SCID), or CID, which are generally less profound than SCID [3]. Mutations in recombinase activating genes 1 and 2 (*RAG1/2*), located in the human chromosome 11p13, represent approximately 20% of all SCID patients [4, 5]. The products of these genes, RAG1 and RAG2 proteins, are essential for V(D)J rearrangement of the antigen receptors during lymphocyte development [4]. Since the first deleterious mutations in *RAG* genes were identified by Schwarz in 1996 [6], more than 200 variants have been described in human patients. The clinical severity partially depends on the level of impairment in the recombinase activity of RAG1/2. Homozygous or compound heterozygous mutations in *RAG1* or *RAG2* may result in null recombination activity and lead to the most severe clinical and immunological phenotypes, highlighted by the absence of T and B lymphocytes. By contrast, in patients carrying homozygous or compound heterozygous missense mutations, the recombinase activity is severely reduced but not absent, and patients may develop leaky SCID or its inflammatory variant, Omenn syndrome (OS).

A spectrum of less-severe clinical and immunological manifestations is now recognized, including combined immunodeficiency with granulomas, common variable immunodeficiency, autoimmunity, and antibody deficiency [7-11]. Moreover, these manifestations can appear early in childhood or during adolescence. These atypical SCID phenotypes have provided unique models to understand the genesis and mechanisms of autoimmunity and other immunological aspects. Here, we present six patients from unrelated families with missense variants in *RAG1* or *RAG2*. Phenotypes observed in these patients ranged from Omenn syndrome to severe mycobacterial infections and

granulomatous disease. In addition, we report the first evidence of two variants not previously associated with immunodeficiency.

Methods

Patients

Peripheral blood mononuclear cells (PBMC) were obtained from patients after securing informed consent that was approved by the local ethics committees in accordance with the Declaration of Helsinki (Protocols 00,165 and 049/2013). The study was multicentric and was conducted from January 2017 to December 2019. All pediatric patients recruited in this study presented with clinical manifestations associated with primary immunodeficiencies.

Mutations Analyses at the RAG-1 and RAG-2 Loci

Genomic DNA was extracted from whole blood and analyzed via whole-exome sequencing as described elsewhere [12]. All mutations were confirmed by Sanger sequencing. The *RAG1* gene was amplified in 2 segments (94–1852 and 1781–3262), and the *RAG2* gene was amplified in one segment (1201–2922). Sequencing was performed directly on the polymerase chain reaction (PCR) products by using the same set of primers. Genetic studies were performed only in patients.

Protein Modeling

Structural models for the core regions of RAG1 and RAG2 are available in the Protein Data Bank (rcsb.org; [13]) for mouse [14-17], zebra fish [18, 19], and lancelet [20] proteins, with resolutions ranging from 2.75 to 4.6 Å. In order to determine whether the relative orientation of RAG1 and RAG2 changes depending on the type of RAG-DNA complex, each RAG1-RAG2 dimer was superimposed in VMD [21] using STAMP [22] in MultiSeq [23] against each RAG1-RAG2 dimer in the apo mouse RAG structure (PDB-ID 4WWX). The RAG1-RAG2 core human models were built in SwissModel [24], using structure 5ZDZ (chains A and B) as reference. As the mutations are located far from each other in the structure of the RAG1-RAG2 complex (Figure S1A and S1B), one multiple mutant model was constructed, containing all the mutations except RAG2-H481D. The RAG2-H481D mutation lies in the plant homeodomain (PHD) domain at the C-terminal region of RAG2. Its structure was solved by X-ray crystallography [25], both as an apo form and in complex with modified histone-3 peptides. The wild-type and mutant human PHD domains were built with SWISS-MODEL [24], using structure 2V87 (chain A) as template (Figure S1C). The models include residues 414–487 for RAG2. Hydrogen atoms were added in CHARMM-GUI [26], taking care that zinc-binding atoms had the appropriate protonation; the structures were energy-minimized in CHARMM45 [27, 28]. The energy-minimized structures were analyzed in RAMPAGE [29] to detect residues in forbidden regions of the Ramachandran plot.

Clinical Classification of the RAG1 and RAG2 Variants

Variants were classified using the criteria in the Standards and Guidelines for the Interpretation of Sequence Variants developed by the American College of Medical Genetics and Genomics (ACMG) and the Association for Molecular Pathology [30]. The information available in public databases and literature was also considered for the final classification of

each variant. The effect of the mutation was evaluated using several algorithms: PolyPhen2 [31], SIFT [32], PredictSNP [33], VarSite [34], REVEL [35], and PON-P2 [36] (Table S1). Except for PolyPhen2 and SIFT, the others are consensus predictors, which use the output from individual programs as part of their training procedure to distinguish damaging from benign changes. ProTSPoM [37] and Missense3D [38] are strictly structural predictors, which analyze the effect of the mutation in the context of available or modeled structures, respectively.

T Lymphocytes Subsets and Proliferation Assays

Peripheral blood mononuclear cells (PBMCs) were isolated using Ficoll density separation (GE healthcare, Life Systems). For the evaluation of different lymphocyte subsets, PBMCs were stained with the following fluorochrome-conjugated monoclonal antibodies against the following cell surface markers: CD3 FITC (Biolegend, clone OKT3), CD4 PE (Biolegend, clone OKT4), CD8 APC (Biolegend, clone SK1), CD19 PerCP-Cy5 (Biolegend, clone 4G7), CD56 APC (Biolegend, clone 5.1H11), CD45 RA PE (Biolegend, clone HI100), and CD45 RO APC (Biolegend, clone UCHL1). For proliferation assays, PBMCs were stained with CellTracker™ green CMDFA dye (ThermoFisher Scientific, USA). Cells were stimulated with purified anti-CD3 plus anti-CD28 antibodies (BioLegend, USA) or PHA (Sigma) for 5 days at 37 °C 5% CO_2. Before sample acquisition, PBMCs were stained using the murine PE-conjugated monoclonal antibody against human CD3 (Biolegend, clone OKT3). All samples were acquired on FACSCanto II (BD bioscience) and analyzed with the use of FlowJo 7.6.5 software (Tree Star, Ashland, OR).

Results

Case 1

Patient was a 2-month-old girl born to consanguineous parents. She was referred to a local hospital for bilateral otorrhea, eczema, and generalized seborrheic dermatitis. Family history included 3 dead siblings. Before hospitalization, the patient had received the BCG and the Hepatitis B vaccines, with no apparent complications. Upon admission, physical examination found abundant purulent discharge from the ears, and generalized dermatitis with desquamation, erythema, and pruritic maculopapular lesions. At age 3 months old, the patient presented with bilateral purulent otic secretions, hepatosplenomegaly, and diarrhea. At 4 months old, she developed rhinorrhea and cough, which persisted 1 month later despite oral antibiotics treatment. Treatment was started with monthly intravenous immunoglobulin (IVIG) replacement therapy and prophylaxis with trimethoprim/sulfamethoxazole (TMP/SMZ) and fluconazole. The patient died of sepsis after HSCT-related complications. Immunological work-up revealed low to undetectable serum levels of immunoglobulins and lymphopenia (Table S2). The patient was classified as OS. A homozygous missense variant (rs148508754) in exon 2 of RAG2 (*RAG2* NM_000536 c.104G > T, p. G35V) was revealed by targeted exome sequencing. This variant is classified as likely pathogenic according to the ACMG criteria (ClinVar Allele ID 488,119). This variant has been reported previously, and when expressed heterologously, it is incapable of promoting recombination [39-44] (Table S3). RAG2-G35 lies in the first Kelch repeat (Figure S1B) at the center of a loop with very specific conformational requirements, which enable the interaction of RAG1-E669 with

the peptide bond NH group of RAG2-G35 (Fig. 1a). This conformation is buttressed by RAG2-Q33, which forms hydrogen bonds to two consecutive peptide bond carbonyls (broken black lines in Fig. 1a). Mutation to V35 results in steric clashes within RAG2 and with RAG1 (Fig. 1b, red broken lines). The sidechain of V35 bumps against the beta carbon of RAG1-H668, a clash that could be relieved by separating RAG1 from RAG2 but would debilitate the complex. Within RAG2, there are clashes with the backbone of V35, a consequence of this residue lying in a forbidden region of the Ramachandran plot. There is also a clash with the amino group of RAG2-K37, which can be eliminated by rotating this particular sidechain, as seen in some structures of RAG2 from zebra fish. Rotating the sidechain of V35 does not eliminate the clashes with the backbone of RAG2 and with RAG1-H668. The mutation can be found in healthy people, but at a very low frequency and as a heterozygote [45]. Regarding the neighboring residues, mutations RAG2-Q33E and RAG1-H668Y are benign according to dbSNP [46] and gnomAD, whereas mutation of RAG1-E669 to K or G causes Omenn syndrome or SCID, respectively [47].

Case 2

Patient is a 3-month-old boy born to non-consanguineous parents who was referred to a local hospital for acute diarrhea. He has two healthy older siblings and tolerated the BCG vaccine at birth. Past medical history included eczema, cow's milk protein-induced proctocolitis, skin rash, adverse drug reactions, at least four previous hospitalizations to treat urinary tract infections, and sepsis. While hospitalized, patient developed bilateral otitis media, seborrheic dermatitis, severe anemia, and recurrent upper respiratory tract infections. Patient died of sepsis while waiting for HSCT. Laboratory work-up showed low levels of serum immunoglobulins and lymphopenia (Table S2). Exome sequencing revealed two missense variants in *RAG2* (NM_000536.4 c.464 T > C p.L155P, and c.685C > T, p.R229W, rs765298019). L155P is predicted as likely pathogenic according to ACMG, it has been reported once in the ClinVar database (ClinVar Allele ID 408,347) and is classified as likely pathogenic but the associated phenotype was not specified. R229W is classified as likely pathogenic according to ACMG criteria, and it is has been reported several times in association to RAG2 deficiency but no activity assay has been published yet [41, 42, 48-52] and Table S3.

RAG2-L155 lies at the core of the third Kelch repeat in RAG2 (Figure S1B), snugly fitting into a hydrophobic and aromatic box, connecting with its sidechain the beta sheet of its repeat with that of the previous one by interacting with RAG2-H94 (Fig. 2a). Upon mutation to P, many of these interactions are lost (Fig. 2b). This repeat includes the longest loop in RAG2, protruding towards RAG1 in the complex (Figure S1A, RAG1-loop), and changes in the packing of residue 155 could alter either the conformation or the position of this loop, affecting the interaction with RAG1. This variant has not been associated with OS or SCID and can be tolerated as heterozygous (gnomAD). On the other hand, the double mutant V154A/L155A is inactive [53], suggesting that the packing of this Kelch repeat is important for function. RAG2-R229 lies at the border between two Kelch repeats (repeat 4 and 5, Figure S1B) engaging in aromatic interactions with RAG2-H222 and a salt bridge with RAG2-E280 and also forms a salt bridge with RAG1-D549 (Fig. 3a). It appears, therefore, important for the structural stability of RAG2 and also for interacting with RAG1. Mutation

to W eliminates the possibility of salt bridges and also increases the distance to RAG1-D549 (Fig. 3b). The fact that each of these two mutations is tolerable as heterozygous (Supplementary Table 3), the phenotype observed in the patient may be explained as a consequence that both variants are in *trans*. In addition, no haploinsufficiency has been shown for RAG1/2, which suggests that the probability of both variants is in *cis* is low, as that would leave one wild-type allele in the patient. Thus, our data suggest that this patient has two defective copies of RAG2, albeit for different reasons: RAG2-L155P destabilizes RAG2 altering the long loop that contacts RAG1, while RAG2-R229W eliminates an important salt bridge connecting to RAG1 and may also destabilize RAG2.

Cases 3 and 4

Patient number 3 is a 13-year-old male, born to consanguineous parents. The patient was referred to a local hospital for a history of recurrent infections, starting before 1 year old. Perinatal history had been uneventful; he received the BCG vaccine at birth, with no adverse reactions. Infections included respiratory, gastrointestinal, oral candidiasis, and herpetic stomatitis. At age 4, after multiple antibiotic treatments, he underwent tympanic ventilation tube placement and adenotonsillectomy. He also developed mild anemia and bronchiectasis as complications. At age 10, he suffered from ganglionar tuberculosis, for which he received a four-drug antimycobacterial regimen for 3 months (maintenance for a year with 2 drugs). At age of 12, he developed gallstones and underwent cholecystectomy, and at age 16, he was treated for chronic diarrhea and abdominal tuberculosis. On physical examination, he had growth failure and malnutrition, with a body mass index below the fifth percentile, non-palpable lymph nodes, and bilateral cracking rales on chest auscultation. High-resolution chest CT scan confirmed extensive bilateral bronchiectasis. Laboratory work-up showed low serum levels of IgG subclasses and persistent lymphopenia. It is important to notice that patient displayed the presence of both T and B lymphocytes; however naive T cells were absent. (Table S2 and Fig. 4A). As shown in Fig. 4B, the CFSE lymphocyte proliferation assay in response to PMA/ionomycin, PHA, and anti-CD3/CD28 was impaired after 5 days compared to healthy control. He was treated since age 13 with intravenous immunoglobulin (IVIG) and oral antibiotic (trimethoprim/sulfamethoxazole and itraconazole) prophylaxis. The patient is alive but has been lost to follow up.

Patient number 4 is a 6-year-old girl, born to non-consanguinous parents, referred to a local hospital with chronic lung disease and skin ulcers, with suspected SCID. Her parents are unrelated from patient number 3. She has three healthy siblings and received the BCG vaccine at birth, with no apparent adverse reactions. She started at age 4, with chronic dry cough in bouts, and a feeling of weakness. At age 5, she developed an erythematous papular lesion in one of her fingers. She was first hospitalized for pneumonia at age 6. Papules had turned into oval-shaped ulcers 10 to 50 mm in diameter, covering her right arm, face, both legs, and buttocks, over the course of a year; she also developed discolored disseminated lesions typical of vitiligo in her eyelids and chest. Other manifestations included an eye granuloma, herpetic stomatitis, pansinusitis, and bilateral bronchiectasis. Physical examination confirmed skin lesions including discolored patches, round ulcers, and scars, as well as short stature, undernutrition, and a temperature of 38 °C, with mild polypnea, dental cavities, bilateral non-tender cervical lymphadenopathy of around 15 mm, and bilateral

rhonchi and rales on auscultation. She was diagnosed with skin tuberculosis, vitiligo, pansinusitis, and bronchiolitis obliterans and started treatment with a 4-drug oral antibiotic regimen, IVIG, and supplementary oxygen overnight, with a provisional diagnosis of combined immunodeficiency. She was hospitalized for pneumonia and died of refractory septic shock at age 8. Blood counts reported low serum immunoglobulin levels and lymphopenia (Table S2). Flow cytometry for lymphocyte subsets showed a $T^{-}B^{-}NK^{+}$ phenotype (Fig. 4A). Lymphoproliferation was impaired for PMA/ionomycin, phytohemagglutinin, and anti-CD3 plus anti-CD28 stimuli (Fig. 4B).

For patients 3 and 4, targeted exome sequencing revealed the same homozygous missense mutation in exon 3 of RAG2(NM_000536.4):c.1441C > G, (p.His481Asp) (rs762054841), a rare variant affecting a codon conserved across species. This variant is predicted as likely pathogenic, according to ACMG criteria. It is absent from the ClinVar database (as of August 2020). A different missense mutation at the same amino acid position (p. H481P) has been previously reported affecting that codon in a Swedish patient with a $T^{-}B^{-}$ SCID phenotype [54]. RAG2-H481 is one of the zinc-binding residues in the PHD domain (Figure S1C), in a Cys_2-His_2 binding site that lies directly below the dimethylated arginine residue of the histone-3 peptide. This suggests that correct assembly of this site is important for histone recognition and binding. Close inspection of nearby residues shows that RAG2-H448 and RAG2-E480 are also within range to participate in zinc binding (Fig. 5a). Mutation to D generates a Cys_2-His-Asp binding site (Fig. 5b), which is also possible but much less frequent [55], and is probably a less avid binding site, given the lower affinity of carboxylates for zinc, compared to imidazole or thiolates [56]. It was recently shown for a RanBP2-type zinc finger [57] that having nearby sidechains that can compete for zinc binding renders the complex kinetically unstable. This could be at work for this mutation, where residues 448, 480, and 481 would compete for zinc binding, wrecking the proper geometry of this binding site and of the histone-binding surface at the opposite side of the beta sheet. That zinc binding is important as shown by the fact that mutation of RAG2-C446 and C478 to W or Y, respectively, cause SCID (HMGD); only RAG2-C478Y is found in gnomAD and tolerated as a heterozygote.

Case 5

The patient is a 1-year-old female from a non-consanguineous family who tolerated the BCG vaccine. Since 22 days of age, she suffered from diarrhea, receiving changes in infant formulas with no improvement. The patient was passing four to five daily stools, associated with the appearance of oral white ulcers with erythematous borders in the oropharynx, inner cheeks, and under the tongue. She was treated with acyclovir without improvement. Subsequently, she developed a perianal abscess, urinary tract infection, and anemia. She was hospitalized and treated with several intravenous antibiotic regimens. Laboratory work-up showed low levels of serum immunoglobulins and lymphopenia (Table S2). The patient received a haploidentical stem cell transplant at age 9 months old, and 1 year later, she is in a good health with 100% donor chimerism and full immune reconstitution. Whole-exome sequencing revealed a homozygous variant in exon 2 of *RAG1*, RAG1(NM_000448.3):c.2291G > C, (p.Arg764Pro), a position highly conserved across mammals, including humans and primates. This variant is predicted as likely pathogenic by

ACMG, and it is absent of gnomAD. RAG1-R764 lies at the C-terminus of an alpha helix in RAG1, facing the second Kelch repeat of RAG2 (Figure S1A and S1B). It engages in a salt bridge and a hydrogen bond with RAG2-E126 and RAG2-Y108, respectively. Another salt bridge with RAG1-E761, in the preceding turn of the alpha helix, stabilizes the complex (Fig. 6a). The Arg-764Pro variant causes loss of all these interactions and the additional loss of a backbone hydrogen bond between the amide NH group of residue 764 and the CO group of residue 760 in the alpha helix (Fig. 6b). This mutation destabilizes both RAG1 and the complex with RAG2. It was described in a heterozygous patient that had three different mutations, two of which rendered inactive RAG [58]. RAG1-R764P is not functional and is expressed at a lower level than the wild type (70%), along the line of our structural interpretation. Regarding the residue neighbors, a mutation of RAG2-E126 to Q or to R is benign (gnomAD), indicating that other sidechains may fill in the gap left by this residue.

Case 6

A 3-month-old female infant was brought for a history of severe atopic dermatitis, chronic perforated otitis media, and recurrent oral candidiasis. Family history was significant for consanguinity and early deaths where the proband's sister had died of septic shock following severe pneumonia. On physical examination, a ruptured eardrum was confirmed, together with extensive severe eczema, oral white plaques, and absent tonsils and lymph nodes. Omenn syndrome in the context of SCID was suspected, and the patient was started on oral antibiotic prophylaxis, together with monthly IVIG. Laboratory work-up showed low levels of serum immunoglobulins and lymphopenia (Table S2). She underwent haploidentical HSCT at age of 4-month-old and full donor chimerism with complete immune reconstitution was achieved. Patient is healthy.

Genetic diagnosis was confirmed through WES after the successful transplant: a deleterious homozygous missense variant in exon 2 of *RAG1* (c.1871G > A, R624H). It is registered in ClinVar and predicted to be probably damaging by PolyPhen and deleterious with low confidence by SIFT. Of the six reported mutations of this work, this is the most frequent one in gnomAD (12 heterozygotes, from different parts of the world). This mutation has been reported previously [6, 43, 59], as a variant with severe reduction in activity when assayed in vitro, but with comparable expression levels as the wild type (Table S3). The mutation is tolerated as heterozygous with a functional allele. R624 lies within a beta sheet that partially covers the alpha helix where one of the catalytic residues (E965) resides (Fig. 7a). Its long sidechain allows the guanidinium nitrogens to engage in hydrogen bonds that stabilize the position of two catalytic residues (E965 and D603), via interactions with both the mainchain and sidechain of N964. Upon mutation to histidine, all these interactions are lost (Fig. 7b), suggesting that the active site would have a different orientation, resulting in lower activity.

Discussion

We have described a series of six patients from unrelated families harboring missense pathogenic variants in recombinase genes: 2 in *RAG1* and 4 in *RAG2*. Two of those variants in *RAG2* (L155P and H481D) were not previously associated with SCID phenotypes. According to gnomAD, these two variants have only been identified in Latino individuals.

Interestingly, although patients 3 and 4 carried the same *RAG2* H481D variant, they did not display the same phenotype. Whereas both patients displayed respiratory diseases including bronchiectasis, only patient 4 presented autoimmune manifestations such as vitiligo and granuloma. In addition, in contrast to patient 4, the presence of B cells was more permissive in patient 3. The causes for these differences remain to be elucidated. From all variants described in this report, the allele frequency of the R624H variant is the highest; however, only one patient described in the literature expressed this variant as homozygous. Three patients presented with a phenotype of Omenn syndrome, one with SCID, and two with CID. According to recent literature, autoimmune hemolytic anemia is the most common autoimmune manifestation in patients with RAG deficiency [7, 60]. Three out of our 6 patients presented anemia, although further studies are needed in order to determine whether this was autoimmune. Both patients with RAG1 deficiencies were successfully transplanted during their first year of life and are currently alive and healthy; by contrast, three of the RAG2 deficient patients have died, and the last one is lost to follow-up. For patient 3, the presence of extensive bilateral bronchiectasis is in line with recent findings in most adult patients with RAG deficiency, where the organ-specific manifestations are most common; however, a concern for successful HSCT due to progressive pulmonary diseases should be also noticed [61]. In CVID, hypomorphic RAG deficiencies, and other inborn errors of immunity, chronic lung disease may result in lung fibrosis and destruction even after adequate immunoglobulin replacement therapy (IGRT). Despite reductions in mortality and pneumonia, granulomatous-lymphocytic interstitial lung disease (GLILD) is an ongoing inflammatory (non-infectious) complication that leads antibody-deficient patients to a decline in lung function. While IGRT supplies these patients with IgG to prevent most infections, the absence of secretory IgA and pentameric IgM in the bronchial surface allows for subclinical infections and chronic inflammation. The incidences of bronchiectasis and chronic obstructive lung disease increase with age in patients with antibody or combined deficiencies. Continued vigilance, early antibiotic treatment for purulent infections, and immunosuppressive therapy directed at T and B cells (azathioprine/rituximab) may be needed to counteract the progression of chronic lung disease and possibly improve HSCT outcome [62].

In Mexico, the BCG vaccine is routinely administered in all children at birth. A high frequency of BCG infection has been reported among RAG deficient SCID patients [63]. Notwithstanding, we did not document BCG complications in our cohort. In retrospect, the presence of chronic cutaneous granulomas with ulceration in our patient 4 could have been associated with rubella virus vaccine (RuV), a known complication of RAG deficiency patients [64], although special RuV immunohistochemical staining techniques were not performed.

In addition to a previous report describing only one patient with RAG2 deficiency [65], this is to our knowledge, the first case series of RAG1 or RAG2 deficient patients from Mexico and Latin America. Although the sample size is small by any standard, we were able to show the wide clinical spectrum of RAG deficiency (Omenn syndrome, CID, and typical SCID), as well as the structural modeling and in silico analysis of the protein consequences for the different variants. Moreover, for the two pathogenic variants that had not been previously

associated with SCID, we were able to show abnormal T cell function as evidenced by impaired cell proliferation.

Biallelic missense germline variants in RAG1 and RAG2 can impair RAG function for many different reasons. Destabilizing the proteins results in lower amounts of working enzyme, and these are made in scant amounts as it is [66]. Weakening the interaction between RAG1 and RAG2 can also reduce the amount of working enzyme. While both RAG1 and RAG2 can bind DNA independently [67], RAG1 is 10 to 100 times less active in the absence of RAG2, and it does not follow the 12/23 rule, leading to aberrant recombination events [66]. Recruiting RAG to active chromatin is the function of the PHD domain, and it also increases both DNA binding and catalysis [68]. Five of the six patients described in this work have alterations in one or more of these processes: RAG1-R764P destabilizes RAG1; RAG2-L155P, −R229W, and −H481D destabilize RAG2; RAG1-R764P, RAG2-G35V, and RAG2-R229W destabilize the RAG1-RAG2 complex; and RAG2-H481D destabilizes the interaction with histones. Another important reason for poor function is the inability to assemble the active site, which is the case for patient six. Other reasons for poor function include alterations in the contact surface with DNA, or in RAG1-RAG2 interactions, but as the mutations in our patients lie far from these sites (Supplementary Fig. 1), we did not entertain these mechanisms as the reason for disease.

All six patients were diagnosed and treated in the three largest cities in Mexico. We need to improve awareness, to increase the referrals of inborn errors of immunity, especially for SCID, a pediatric emergency, to provide gene consulting and genetic studies in other members of the family. Moreover, the addition of biomarkers such as the detection of antibodies to cytokines, a decreased presence of TCRV7.2a^{+} MAIT cells, or a skewed B and T cell repertoire, may facilitate clinicians in the diagnosis of combined immunodeficiencies. In Mexico and Latin America, a few regions are known to practice consanguineous marriages, although a more frequent occurrence is a high degree of inbreeding in closed, geographically, or culturally isolated communities of less than 1000 inhabitants. Known consanguinity, a family history of early deaths, severe adverse reactions to the BCG vaccine, and an early onset of recurrent infections are all well-known red flags that should raise the suspicion for SCID phenotypes, including those that result from RAG deficiency. We have yet to implement newborn screening for SCID in our country to identify patients with the most severe form of inborn errors of immunity during their first month of life, before infectious and non-infectious complications ensue, and increase the chances of a successful HSCT.

In conclusion, here, we presented six patients with *RAG1/2* mutations. All were missense variants, and therefore, some residual recombinase V(D)J activity may have been present. For the case of *RAG2*, three variants were in the core domain, and one in the PHD domain, whereas the variants identified in *RAG1* were found in the zinc-binding domain and adjacent to the catalytic site, respectively. As previously reported, the broad spectrum of phenotypes associated with *RAG1/2* variants depends on the position of mutations and how these impact recombinase V(D)J activity. Consequently, information on repertoire diversity in T lymphocytes and their phenotypes will be of interest to understand how RAG1/2 pathogenic variants may result in the broad spectrum of clinical manifestations seen in *RAG* deficiency.

Supplementary Material

Refer to Web version on PubMed Central for supplementary material.

Acknowledgements

The authors would like to thank the patients and their families for participating in this study.

Funding

MECM is supported by Consejo Nacional de Ciencia y Tecnología (CONACYT 281854).

LDN is supported by the Division of Intramural Research, National Institute of Allergy and Infectious Diseases, National Institutes of Health, Bethesda, MD, USA.

References

1. Sponzilli I, Notarangelo LD. Severe combined immunodeficiency (SCID): from molecular basis to clinical management. Acta Biomed. 2011;82(1):5–13. [PubMed: 22069950]
2. Fischer A Severe combined immunodeficiencies (SCID). Clin Exp Immunol. 2000;122(2):143–9. [PubMed: 11091267]
3. Tangye SG, Al-Herz W, Bousfiha A, Chatila T, Cunningham-Rundles C, Etzioni A, et al. Human inborn errors of immunity: 2019 Update on the Classification from the International Union of Immunological Societies Expert Committee. J Clin Immunol. 2020;40(1):24–64. [PubMed: 31953710]
4. Notarangelo LD, Kim MS, Walter JE, Lee YN. Human RAG mutations: biochemistry and clinical implications. Nat Rev Immunol. 2016;16(4):234–46. [PubMed: 26996199]
5. Dvorak CC, Haddad E, Buckley RH, Cowan MJ, Logan B, Griffith LM, et al. The genetic landscape of severe combined immunodeficiency in the United States and Canada in the current era (2010–2018). J Allergy Clin Immunol. 2019;143(1):405–7. [PubMed: 30193840]
6. Schwarz K, Gauss GH, Ludwig L, Pannicke U, Li Z, Lindner D, et al. RAG mutations in human B cell-negative SCID. Science. 1996;274(5284):97–9. [PubMed: 8810255]
7. Delmonte OM, Schuetz C, Notarangelo LD. RAG deficiency: two genes, many diseases. J Clin Immunol. 2018;38(6):646–55. [PubMed: 30046960]
8. De Ravin SS, Cowen EW, Zarember KA, Whiting-Theobald NL, Kuhns DB, Sandler NG, et al. Hypomorphic Rag mutations can cause destructive midline granulomatous disease. Blood. 2010;116(8):1263–71. [PubMed: 20489056]
9. Patiroglu T, Akar HH, Gilmour K, Ozdemir MA, Bibi S, Henriquez F, et al. Atypical severe combined immunodeficiency caused by a novel homozygous mutation in Rag1 gene in a girl who presented with pyoderma gangrenosum: a case report and literature review. J Clin Immunol. 2014;34(7):792–5. [PubMed: 25104208]
10. Schuetz C, Huck K, Gudowius S, Megahed M, Feyen O, Hubner B, et al. An immunodeficiency disease with RAG mutations and granulomas. N Engl J Med. 2008;358(19):2030–8. [PubMed: 18463379]
11. Villa A, Notarangelo LD. RAG gene defects at the verge of immunodeficiency and immune dysregulation. Immunol Rev. 2019;287(1):73–90. [PubMed: 30565244]
12. Boutboul D, Kuehn HS, Van de Wyngaert Z, Niemela JE, Callebaut I, Stoddard J, et al. Dominant-negative IKZF1 mutations cause a T, B, and myeloid cell combined immunodeficiency. J Clin Invest. 2018;128(7):3071–87. [PubMed: 29889099]
13. Berman HM, Westbrook J, Feng Z, Gilliland G, Bhat TN, Weissig H, et al. The protein data bank. Nucleic Acids Res. 2000;28(1):235–42. [PubMed: 10592235]
14. Kim MS, Lapkouski M, Yang W, Gellert M. Crystal structure of the V(D)J recombinase RAG1-RAG2. Nature. 2015;518(7540):507–11. [PubMed: 25707801]

15. Kim MS, Chuenchor W, Chen X, Cui Y, Zhang X, Zhou ZH, et al. Cracking the DNA code for V(D)J recombination. Mol Cell. 2018;70(2):358–70 e4. [PubMed: 29628308]
16. Chen X, Cui Y, Best RB, Wang H, Zhou ZH, Yang W, et al. Cutting antiparallel DNA strands in a single active site. Nat Struct Mol Biol. 2020;27(2):119–26. [PubMed: 32015552]
17. Chen X, Cui Y, Wang H, Zhou ZH, Gellert M, Yang W. How mouse RAG recombinase avoids DNA transposition. Nat Struct Mol Biol. 2020;27(2):127–33. [PubMed: 32015553]
18. Ru H, Chambers MG, Fu TM, Tong AB, Liao M, Wu H. Molecular mechanism of V(D)J recombination from synaptic RAG1-RAG2 complex structures. Cell. 2015;163(5):1138–52. [PubMed: 26548953]
19. Ru H, Mi W, Zhang P, Alt FW, Schatz DG, Liao M, et al. DNA melting initiates the RAG catalytic pathway. Nat Struct Mol Biol. 2018;25(8):732–42. [PubMed: 30061602]
20. Zhang Y, Cheng TC, Huang G, Lu Q, Surleac MD, Mandell JD, et al. Transposon molecular domestication and the evolution of the RAG recombinase. Nature. 2019;569(7754):79–84. [PubMed: 30971819]
21. Humphrey W, Dalke A, Schulten K. VMD: visual molecular dynamics. J Mol Graph. 1996;14(1):33–8 (27-8). [PubMed: 8744570]
22. Russell RB, Barton GJ. Multiple protein sequence alignment from tertiary structure comparison: assignment of global and residue confidence levels. Proteins. 1992;14(2):309–23. [PubMed: 1409577]
23. Roberts E, Eargle J, Wright D, Luthey-Schulten Z. MultiSeq: unifying sequence and structure data for evolutionary analysis. BMC Bioinformatics. 2006;7:382. [PubMed: 16914055]
24. Bertoni M, Kiefer F, Biasini M, Bordoli L, Schwede T. Modeling protein quaternary structure of homo- and hetero-oligomers beyond binary interactions by homology. Sci Rep. 2017;7(1):10480. [PubMed: 28874689]
25. Ramon-Maiques S, Kuo AJ, Carney D, Matthews AG, Oettinger MA, Gozani O, et al. The plant homeodomain finger of RAG2 recognizes histone H3 methylated at both lysine-4 and arginine-2. Proc Natl Acad Sci U S A. 2007;104(48):18993–8. [PubMed: 18025461]
26. Jo S, Kim T, Iyer VG, Im W. CHARMM-GUI: a web-based graphical user interface for CHARMM. J Comput Chem. 2008;29(11):1859–65. [PubMed: 18351591]
27. Brooks BR, Brooks CL 3rd, Mackerell AD Jr, Nilsson L, Petrella RJ, Roux B, et al. CHARMM: the biomolecular simulation program. J Comput Chem. 2009;30(10):1545–614. [PubMed: 19444816]
28. Lee J, Cheng X, Swails JM, Yeom MS, Eastman PK, Lemkul JA, et al. CHARMM-GUI input generator for NAMD, GROMACS, AMBER, OpenMM, and CHARMM/OpenMM simulations using the CHARMM36 additive force field. J Chem Theory Comput. 2016;12(1):405–13. [PubMed: 26631602]
29. Lovell SC, Davis IW, Arendall WB 3rd, de Bakker PI, Word JM, Prisant MG, et al. Structure validation by Calpha geometry: phi, psi and Cbeta deviation. Proteins. 2003;50(3):437–50. [PubMed: 12557186]
30. Richards S, Aziz N, Bale S, Bick D, Das S, Gastier-Foster J, et al. Standards and guidelines for the interpretation of sequence variants: a joint consensus recommendation of the American College of Medical Genetics and Genomics and the Association for Molecular Pathology. Genet Med. 2015;17(5):405–24. [PubMed: 25741868]
31. Adzhubei IA, Schmidt S, Peshkin L, Ramensky VE, Gerasimova A, Bork P, et al. A method and server for predicting damaging missense mutations. Nat Methods. 2010;7(4):248–9. [PubMed: 20354512]
32. Sim NL, Kumar P, Hu J, Henikoff S, Schneider G, Ng PC. SIFT web server: predicting effects of amino acid substitutions on proteins. Nucleic Acids Res. 2012;40(Web Server issue):W452–7. [PubMed: 22689647]
33. Bendl J, Stourac J, Salanda O, Pavelka A, Wieben ED, Zendulka J, et al. PredictSNP: robust and accurate consensus classifier for prediction of disease-related mutations. PLoS Comput Biol. 2014;10(1):e1003440. [PubMed: 24453961]
34. Laskowski RA, Stephenson JD, Sillitoe I, Orengo CA, Thornton JM. VarSite: Disease variants and protein structure. Protein Sci. 2020;29(1):111–9. [PubMed: 31606900]

35. Ioannidis NM, Rothstein JH, Pejaver V, Middha S, McDonnell SK, Baheti S, et al. REVEL: an ensemble method for predicting the pathogenicity of rare missense variants. Am J Hum Genet. 2016;99(4):877–85. [PubMed: 27666373]
36. Niroula A, Urolagin S, Vihinen M. PON-P2: prediction method for fast and reliable identification of harmful variants. PLoS ONE. 2015;10(2):e0117380. [PubMed: 25647319]
37. Banerjee A, Mitra P. Estimating the effect of single-point mutations on protein thermodynamic stability and analyzing the mutation landscape of the p53 protein. J Chem Inf Model. 2020;60(6):3315–23. [PubMed: 32401507]
38. Ittisoponpisan S, Islam SA, Khanna T, Alhuzimi E, David A, Sternberg MJE. Can predicted protein 3D structures provide reliable insights into whether missense variants are disease associated? J Mol Biol. 2019;431(11):2197–212. [PubMed: 30995449]
39. Meshaal SS, El Hawary RE, AbdElaziz DS, Eldash A, Alkady R, Lotfy S, et al. Phenotypical heterogeneity in RAG-deficient patients from a highly consanguineous population. Clin Exp Immunol. 2019;195(2):202–12. [PubMed: 30307608]
40. Lev A, Simon AJ, Trakhtenbrot L, Goldstein I, Nagar M, Stepensky P, et al. Characterizing T cells in SCID patients presenting with reactive or residual T lymphocytes. Clin Dev Immunol. 2012;2012:261470. [PubMed: 23243423]
41. Sobacchi C, Marrella V, Rucci F, Vezzoni P, Villa A. RAG-dependent primary immunodeficiencies. Hum Mutat. 2006;27(12):1174–84. [PubMed: 16960852]
42. Tabori U, Mark Z, Amariglio N, Etzioni A, Golan H, Biloray B, et al. Detection of RAG mutations and prenatal diagnosis in families presenting with either T-B- severe combined immunodeficiency or Omenn's syndrome. Clin Genet. 2004;65(4):322–6. [PubMed: 15025726]
43. Corneo B, Moshous D, Gungor T, Wulffraat N, Philippet P, Le Deist FL, et al. Identical mutations in RAG1 or RAG2 genes leading to defective V(D)J recombinase activity can cause either T-B- severe combined immune deficiency or Omenn syndrome. Blood. 2001;97(9):2772–6. [PubMed: 11313270]
44. Corneo B, Moshous D, Callebaut I, de Chasseval R, Fischer A, de Villartay JP. Three-dimensional clustering of human RAG2 gene mutations in severe combined immune deficiency. J Biol Chem. 2000;275(17):12672–5. [PubMed: 10777560]
45. Karczewski KJ, Francioli LC, Tiao G, Cummings BB, Alfoldi J, Wang Q, et al. The mutational constraint spectrum quantified from variation in 141,456 humans. Nature. 2020;581(7809):434–43. [PubMed: 32461654]
46. Sherry ST, Ward MH, Kholodov M, Baker J, Phan L, Smigielski EM, et al. dbSNP: the NCBI database of genetic variation. Nucleic Acids Res. 2001;29(1):308–11. [PubMed: 11125122]
47. Cooper DN, Ball EV, Krawczak M. The human gene mutation database. Nucleic Acids Res. 1998;26(1):285–7. [PubMed: 9399854]
48. Luk ADW, Lee PP, Mao H, Chan KW, Chen XY, Chen TX, et al. Family history of early infant death correlates with earlier age at diagnosis but not shorter time to diagnosis for severe combined immunodeficiency. Front Immunol. 2017;8:808. [PubMed: 28747913]
49. Al-Mousa H, Abouelhoda M, Monies DM, Al-Tassan N, Al-Ghonaium A, Al-Saud B, et al. Unbiased targeted next-generation sequencing molecular approach for primary immunodeficiency diseases. J Allergy Clin Immunol. 2016;137(6):1780–7. [PubMed: 26915675]
50. Schuetz C, Neven B, Dvorak CC, Leroy S, Ege MJ, Pannicke U, et al. SCID patients with ARTEMIS vs RAG deficiencies following HCT: increased risk of late toxicity in ARTEMIS-deficient SCID. Blood. 2014;123(2):281–9. [PubMed: 24144642]
51. Safaei S, Pourpak Z, Moin M, Houshmand M. IL7R and RAG1/2 genes mutations/polymorphisms in patients with SCID. Iran J Allergy Asthma Immunol. 2011;10(2):129–32. [PubMed: 21625022]
52. Villa A, Sobacchi C, Notarangelo LD, Bozzi F, Abinun M, Abrahamsen TG, et al. V(D)J recombination defects in lymphocytes due to RAG mutations: severe immunodeficiency with a spectrum of clinical presentations. Blood. 2001;97(1):81–8. [PubMed: 11133745]
53. Gomez CA, Ptaszek LM, Villa A, Bozzi F, Sobacchi C, Brooks EG, et al. Mutations in conserved regions of the predicted RAG2 kelch repeats block initiation of V(D)J recombination and result in primary immunodeficiencies. Mol Cell Biol. 2000;20(15):5653–64. [PubMed: 10891502]

54. Noordzij JG, de Bruin-Versteeg S, Verkaik NS, Vossen JM, de Groot R, Bernatowska E, et al. The immunophenotypic and immunogenotypic B-cell differentiation arrest in bone marrow of RAG-deficient SCID patients corresponds to residual recombination activities of mutated RAG proteins. Blood. 2002;100(6):2145–52. [PubMed: 12200379]
55. Ireland SM, Martin ACR. ZincBind-the database of zinc binding sites. Database (Oxford). 2019;2019:baz006.
56. Krezel A, Maret W. The biological inorganic chemistry of zinc ions. Arch Biochem Biophys. 2016;611:3–19. [PubMed: 27117234]
57. Soni K, Martinez-Lumbreras S, Sattler M. Conformational dynamics from ambiguous zinc coordination in the RanBP2-type zinc finger of RBM5. J Mol Biol. 2020;432(14):4127–38. [PubMed: 32450081]
58. Lee YN, Frugoni F, Dobbs K, Walter JE, Giliani S, Gennery AR, et al. A systematic analysis of recombination activity and genotype-phenotype correlation in human recombination-activating gene 1 deficiency. J Allergy Clin Immunol. 2014;133(4):1099–108. [PubMed: 24290284]
59. Alsmadi O, Al-Ghonaium A, Al-Muhsen S, Arnaout R, Al-Dhekri H, Al-Saud B, et al. Molecular analysis of T-B-NK+ severe combined immunodeficiency and Omenn syndrome cases in Saudi Arabia. BMC Med Genet. 2009;10:116. [PubMed: 19912631]
60. Farmer JR, Foldvari Z, Ujhazi B, De Ravin SS, Chen K, Bleesing JJH, et al. Outcomes and treatment strategies for autoimmunity and hyperinflammation in patients with RAG deficiency. J Allergy Clin Immunol Pract. 2019;7(6):1970–85 e4. [PubMed: 30877075]
61. Lawless D, Geier CB, Farmer JR, Lango Allen H, Thwaites D, Atschekzei F, et al. Prevalence and clinical challenges among adults with primary immunodeficiency and recombination-activating gene deficiency. J Allergy Clin Immunol. 2018;141(6):2303–6. [PubMed: 29477728]
62. Baumann U, Routes JM, Soler-Palacin P, Jolles S. The lung in primary immunodeficiencies: new concepts in infection and inflammation. Front Immunol. 2018;9:1837. [PubMed: 30147696]
63. Kutukculer N, Gulez N, Karaca NE, Aksu G, Berdeli A. Novel mutations and diverse clinical phenotypes in recombinase-activating gene 1 deficiency. Ital J Pediatr. 2012;38:8. [PubMed: 22424479]
64. Perelygina L, Icenogle J, Sullivan KE. Rubella virus-associated chronic inflammation in primary immunodeficiency diseases. Curr Opin Allergy Clin Immunol. 2020;20(6):574–81. [PubMed: 33044342]
65. Dorna MB, Barbosa PFA, Rangel-Santos A, Csomos K, Ujhazi B, Dasso JF, et al. Combined immunodeficiency with late-onset progressive hypogammaglobulinemia and normal B cell count in a patient with RAG2 deficiency. Front Pediatr. 2019;7:122. [PubMed: 31058115]
66. Carmona LM, Fugmann SD, Schatz DG. Collaboration of RAG2 with RAG1-like proteins during the evolution of V(D)J recombination. Genes Dev. 2016;30(8):909–17. [PubMed: 27056670]
67. Oudinet C, Braikia FZ, Dauba A, Khamlichi AA. Recombination may occur in the absence of transcription in the immunoglobulin heavy chain recombination centre. Nucleic Acids Res. 2020;48(7):3553–66. [PubMed: 32086526]
68. Shimazaki N, Tsai AG, Lieber MR. H3K4me3 stimulates the V(D) J RAG complex for both nicking and hairpinning in trans in addition to tethering in cis: implications for translocations. Mol Cell. 2009;34(5):535–44. [PubMed: 19524534]

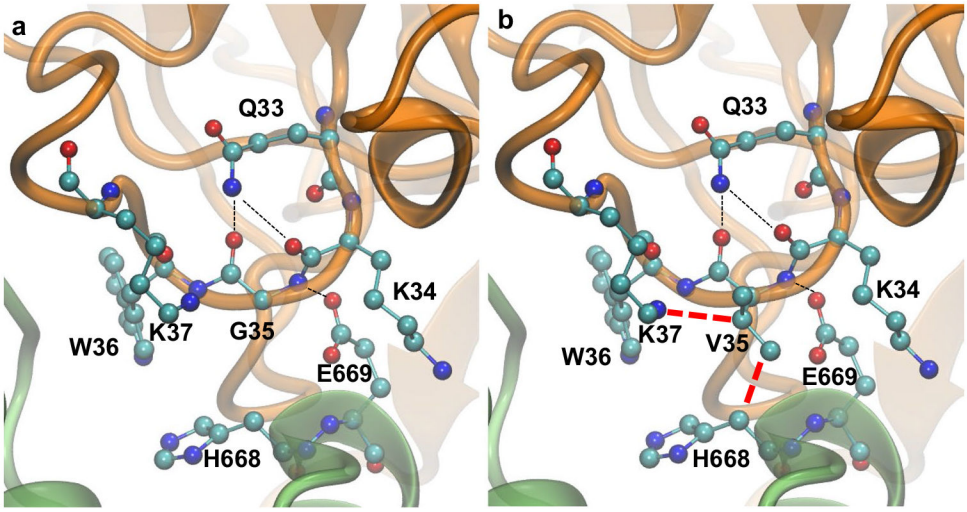

Fig. 1.

Effect of the G35V mutation. RAG1 is shown as a green ribbon and RAG2 in orange, approximately in the same orientation as Supplementary Fig. 1A; all residues are shown in balls and sticks and CPK colors (carbon in cyan, nitrogen in blue, oxygen in red). **a** The wild-type structure, without steric clashes and a network of hydrogen bonds (broken black lines) between the sidechain of Q33 and the backbone carbonyls of G35 and K34, ensuring the right conformation for the interaction of E669 with the backbone amide of G35. **b** The sidechain of V35, engaging in potential clashes (broken red lines) with H668, K37 and its backbone atoms. These clashes cannot be relieved by rotating the sidechain, which would result in a close contact with W36

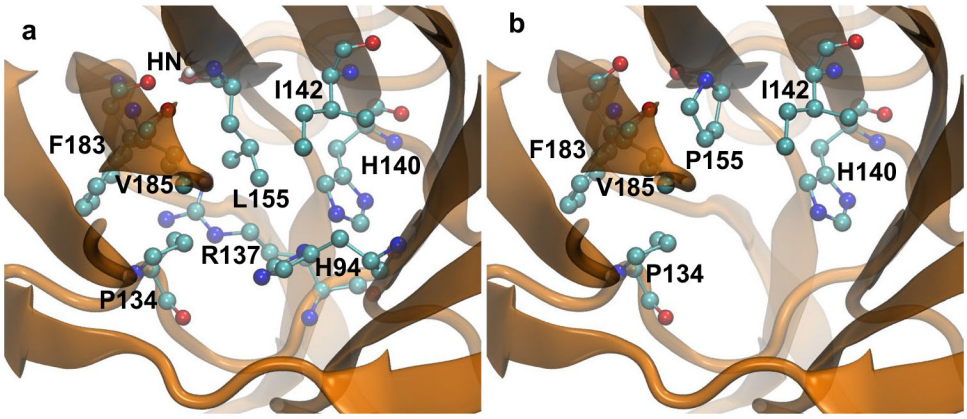

Fig. 2.

Effect of the L155P mutation. RAG2 is shown as an orange ribbon, seen from the top of Supplementary Fig. 1A; all residues are shown in balls and sticks and CPK colors (carbon in cyan, nitrogen in blue, oxygen in red). **a** The hydrophobic and aromatic cage around L155, with interactions that bridge three beta strands in the Kelch repeat and link it to the previous one (through H94). Also, a backbone hydrogen bond, indicated by HN, binds L155 to F183 in the adjacent beta strand. **b** The incomplete cage around P155, lacking H94 and R137, effectively losing interactions with the previous Kelch repeat. Also, the hydrogen bond to F183 is missing, leading to a weakened beta sheet

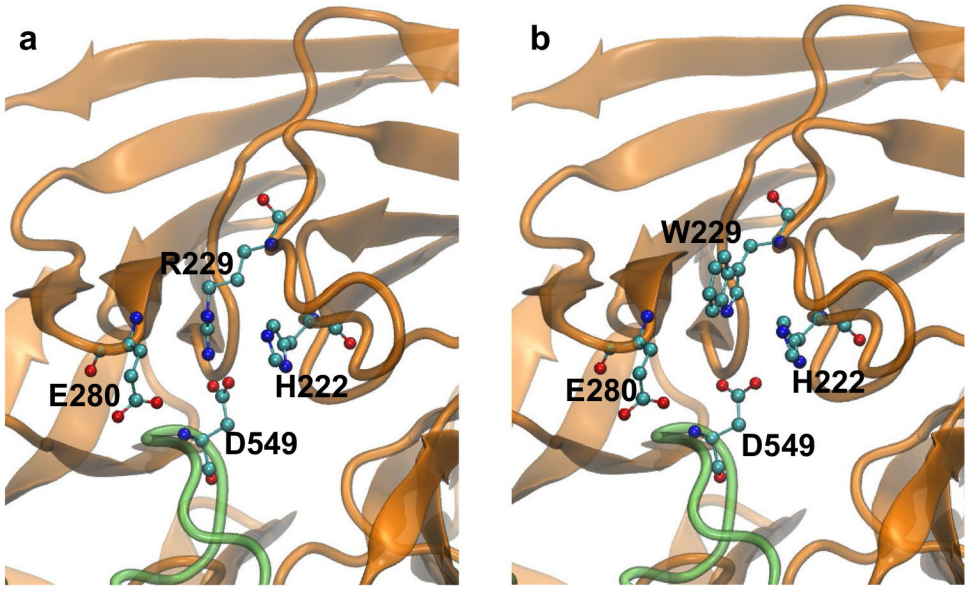

Fig. 3.

Effect of the R229W mutation. RAG1 is shown as a green ribbon and RAG2 in orange, looking at the bottom of RAG2 from the perspective of RAG1; all residues are shown in balls and sticks and CPK colors (carbon in cyan, nitrogen in blue, oxygen in red). **a** The structural role of R229 by interacting with adjacent residues of RAG2 from the previous Kelch repeat (H222) and its own repeat (E280), and its interaction with RAG1 (D549). **b** shows that W229 lies farther away from D549 and E280, losing the possible favorable interactions with them; H222 can still interact with W229 and D549, functioning as a bridge between them

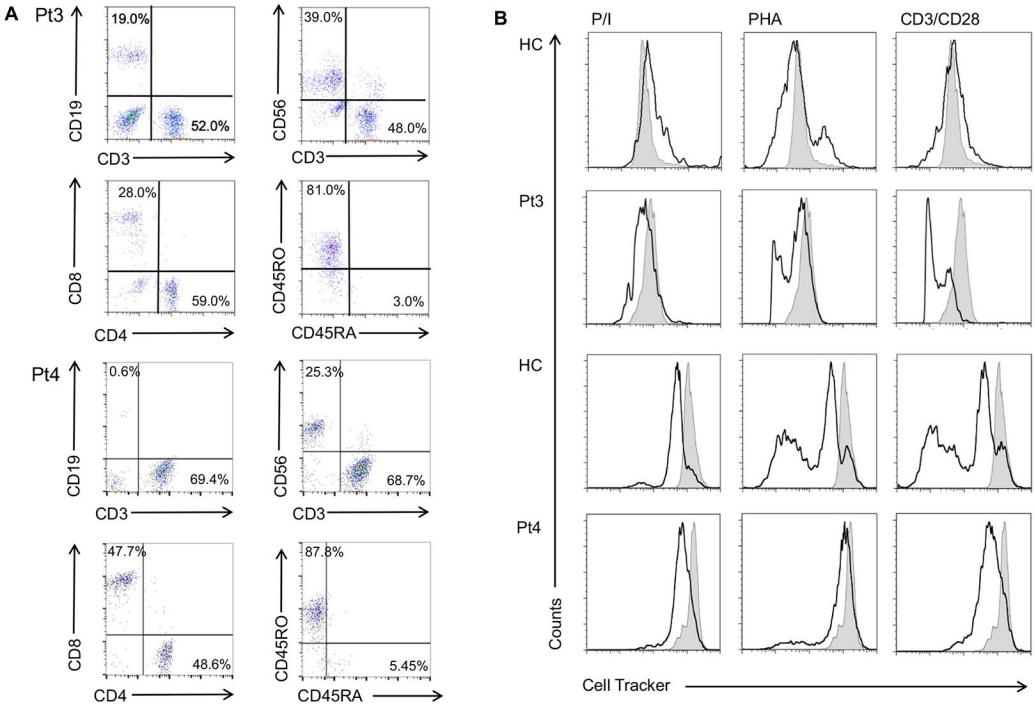

Fig. 4.

A PBMCs were stained with the following panel of fluorochrome-conjugated monoclonal Abs directed against following cell surface markers: CD3 FITC, CD4 PE, CD8 APC, CD19 PerCP-Cy5, CD56 APC, CD45 RA PE, and CD45 RO APC. Then cells were acquired on FACSCanto II (BD bioscience) and analyzed with the use of FlowJo 7.6.5 software (Tree Star, Ashland, OR). **B** PBMCs were subject to proliferation assays by staining PBMCs with Cell-Tracker™ green CMDFA dye (ThermoFisher Scientific, USA), then cells were stimulated with LEAF purified anti-CD3 plus anti-CD28 antibodies (BioLegend, USA) or PHA (Sigma) for 5 days at 37 °C 5% CO_2. Then, PBMCs were stained using the murine PE conjugated monoclonal antibody directed against human CD3. Flow cytometric data were acquired on FACSCanto II (BD bioscience) and analyzed with the use of FlowJo 7.6.5 software (Tree Star, Ashland, OR). Gates were set to include $CD3^+$ lymphocytes. Thereafter, T cells were defined by the expression of CD3

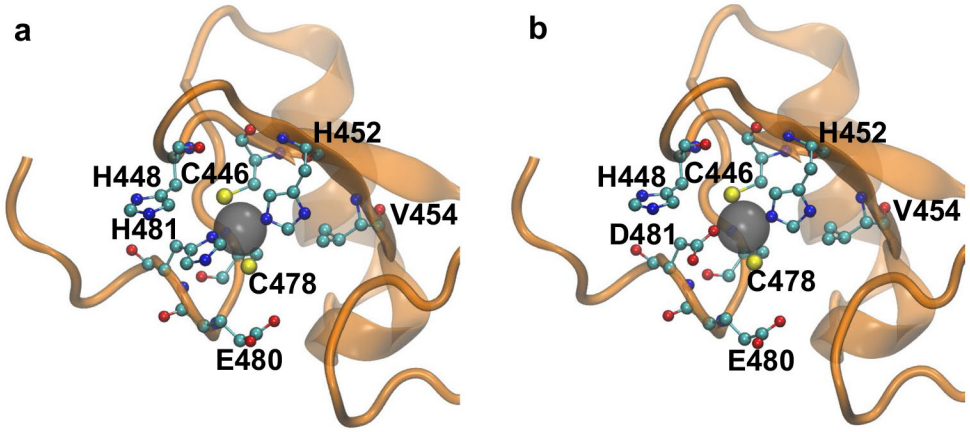

Fig. 5.

Effect of the H481D mutation. RAG2 is shown as an orange ribbon, in the same orientation as Supplementary Fig. 1C. The coordination sphere of Zn2 is shown in balls and sticks; all residues are shown in CPK colors (carbon in cyan, nitrogen in blue, oxygen in red, sulfur in yellow). **a** The wild-type environment of Zn2; **b** the mutation to D481. Noteworthy are the neighboring histidine and glutamate residues, which could compete with D481 for coordinating Zn and make this site kinetically labile

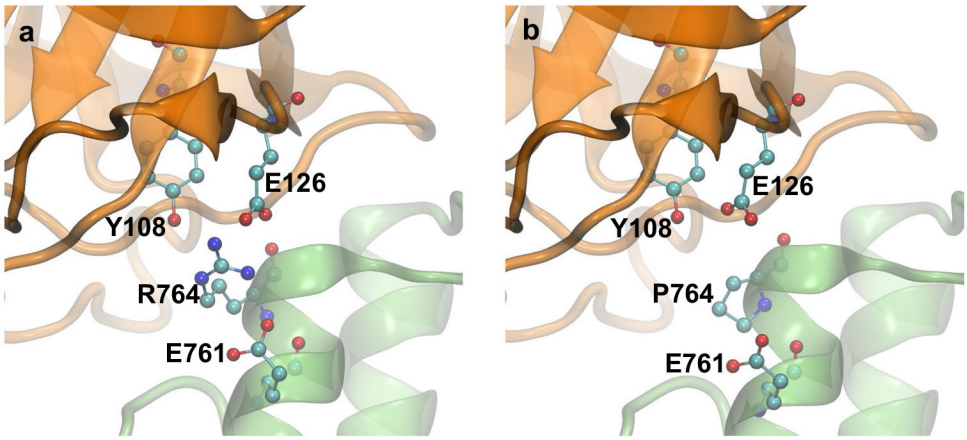

Fig. 6.

Effect of the R764P mutation. RAG1 is shown as a green ribbon and RAG2 in orange, roughly in the same perspective as Supplementary Fig. 1A; all residues are shown in balls and sticks and CPK colors (carbon in cyan, nitrogen in blue, oxygen in red). **a** The hydrogen bond and electrostatic interactions of R764 with Y108 and E126 in RAG2, and E761 one turn below in the alpha helix in RAG1, buttressing the conformation of the sidechain of R764. **b** P764 no longer interacts with any of these sidechains and has also lost the possibility to form a hydrogen bond with its backbone imide, weakening the last turn of the helix

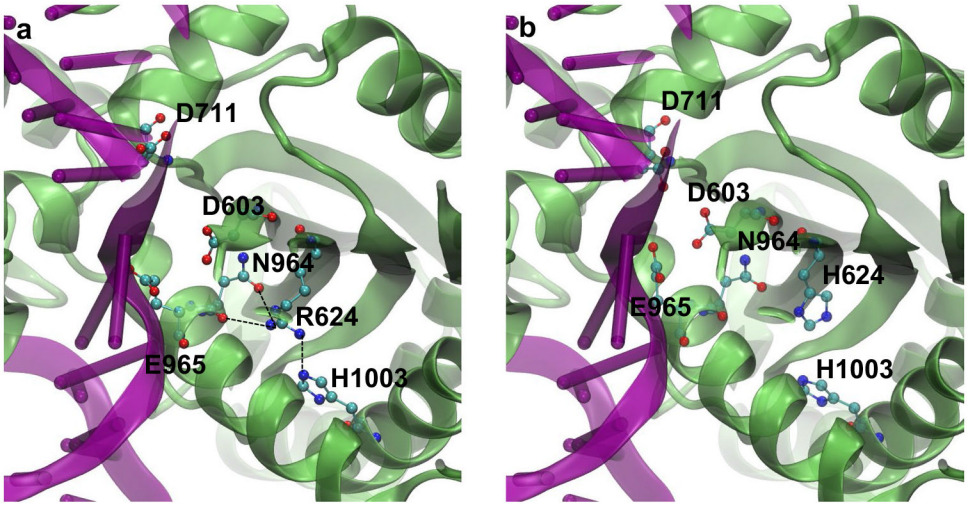

Fig. 7.

Effect of the R624H mutation. RAG1 is shown as a green ribbon and DNA in purple, zooming in at the active site; all residues are shown in balls and sticks and CPK colors (carbon in cyan, nitrogen in blue, oxygen in red). Residues D603, D711 and E965 constitute the active site residues, flanking the nick in the DNA strand. Hydrogen bonds are depicted as black broken lines. **a** The Hydrogen bond and electrostatic interactions of R624 with both the mainchain carbonyl and the sidechain carbonyl of N964, buttressing the position of the helix where E965 resides. R624 also engages in a Hydrogen bond with H1003 from an adjacent helix. N964 could also engage in favorable electrostatic interactions with D603. **b** H624, on account of being shorter, can no longer engage in any of the critical Hydrogen bonds that stabilize the position of the helix that forms part of the active site